High specification CCD-based spectrometry for metals analysis

New developments in hardware and spectrum processing enable the ARL QUANTRIS CCD-based spectrometer to achieve the performance of photo-multiplier tube instruments for the determination of low levels of carbon, nitrogen, sulphur and phosphorus with excellent precision, coupled with an equivalent or superior precision for the measurement of key alloying elements.

Emile Muller, Jean-Marc Böhlen and Edmund Halász
Thermo Electron

The analytical demands of the metal industry are constantly increasing in terms of detection limits, precision, accuracy, speed of analysis and flexibility. More and more metal processors are looking for reliable instruments that can analyse a greater variety of material grades, yet which are flexible and need no hardware modifications for further extensions.

Optical Emission Spectrometry (OES) for elemental analysis of metals offers a high level of performance at extremely high speed, coupled with simple sample preparation and low cost of ownership. Spectrometer manufacturers rapidly adopted solid-state detectors because they allow the design of smaller optics and hence small instruments, like portables and bench tops. Among the solid-state detectors available, charge coupled devices (CCDs) – already becoming an industry standard in digital photography, scientific and medical imaging – were adopted in OES.

However, until recently, it was thought that CCD-based instruments, despite their high versatility, had lower performance in comparison with photo-multiplier tube (PMT) instruments, in particular having higher detection limits and lower precision. PMT-based instruments, however, especially for multi-matrix applications, do have geometric limitations.

This article introduces the ARL QUANTRIS (*Figure 1*) produced by the Thermo Electron Corporation – a second-generation optical emission spectrometer based on CCD technology. New developments in hardware and spectrum processing enable the instrument to achieve the performance of PMT instruments with, for instance, the determination of carbon, nitrogen, sulphur and phosphorus in steels at low levels, and with excellent precision.

● **Figure 1** ***The ARL QUANTRIS CCD-based metals analyser***

Instrument architecture

The instrument has an innovative architecture, built on proven modern technologies and consists of three main modules: the spark stand with the CCS, the optics with the CCD detectors, and the control and readout electronics.

Sample stand and CCS

The analysis stand is water-cooled for better heat evacuation, and has a very low stand-by flow and a fast flush and dust blow-out system. The sample excitation source is the patented Thermo CCS. This source was introduced in 1994 on the high-specification ARL 4460

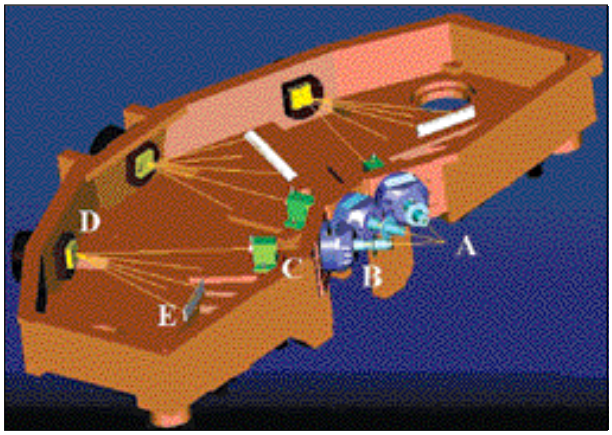

● **Figure 2** *Schematics of the optics of the ARL QUANTRIS*

Flat field spectrograph	Wavelength range (nm)	Grating (groove/mm at grating centre)	Average dispersion (nm/mm)	Average band pass par pixel (pm/pixel)
VUV spectrograph	130-200	3240	1.2	8
Basic spectrograph	200-410	1,105	3.5	24
Optional alkaline spectrograph	410-780	590	6.7	43

● **Table 1** *ARL QUANTRIS optics characteristics*

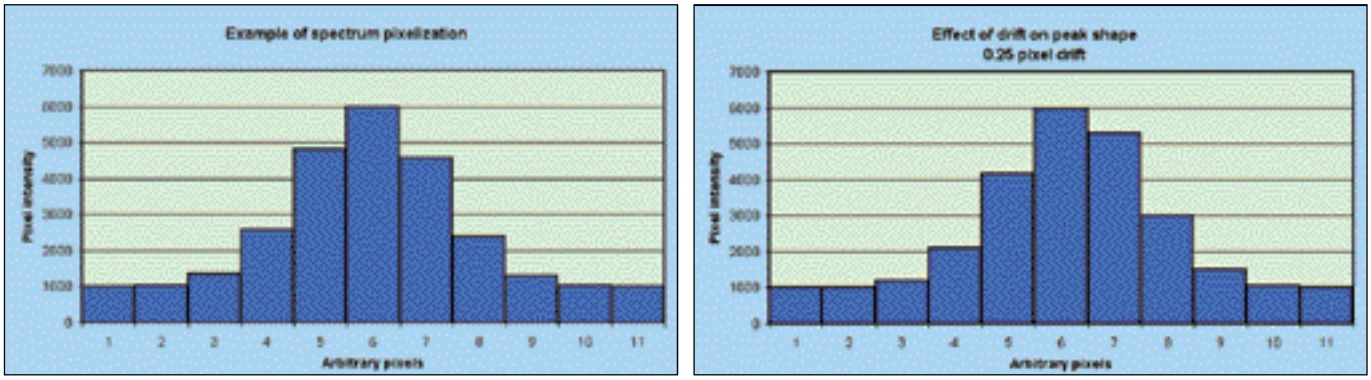

● **Figure 3** *(a) Example of spectrum 'pixelisation', (b) The effect of 0.25 pixel drift to the right on the above spectrum*

PMT spectrometer and this is the first time that such a high-performance source has become available on a CCD-based instrument, offering significant advantages in comparison to any other spark generator currently used for OES. It is the only servo-controlled 'digital source' on the market and its high degree of flexibility enables all analytical figures to be optimised for each type of metal and alloy.

Flat field optics with CCD detectors

The CCD of the ARL QUANTRIS is specifically designed for high-specification industrial, scientific or military applications and has three parallel lines of 8,640 detectors of 7 by 9.8 micrometers. The optics are based on the concept of the flat field spectrograph and consist of a primary slit and a flat field grating that focuses the light onto a plane surface, where a CCD detector is placed. There are three flat-field spectrographs (see *Figure* 2), covering the spectral ranges: 130–200, 200–410 and 410–780nm. Each of them has its own focusing lens and holographic aberration-corrected concave grating, enabling optimised light collection on the high-performance linear CCD. The first spectrograph CCD is covered with a fluorescent coating for increased sensitivity and the detectors are also cooled (with Peltier coolers) and thermo-controlled within ±0.06°C at a temperature close to 0°C.

The middle spectrograph is oriented vertically and the two others horizontally. The letters indicate the position of the light source (A), the lens (B), the primary slit (C), the grating (D), and the CCD (E) of the third spectrograph. The CCD replaces the photomultiplier detectors used in traditional spectrometers and gives the instrument immense flexibility.

The spectrometer body is made of cast iron, operates under vacuum, and ensures excellent short and long-term temperature and ambient pressure stability, together with minimal absorption of light in the ultra-violet (UV) domain.

The characteristics of the optics are shown in *Table 1*. The light is directed to the optics in direct-reading mode. This is a key feature because it eliminates the need for fibre optics that suffer from effects that degrade light transmission such as aging and solarisation.

Control and readout electronics

All instrument functions are monitored and controlled by an internal controller.

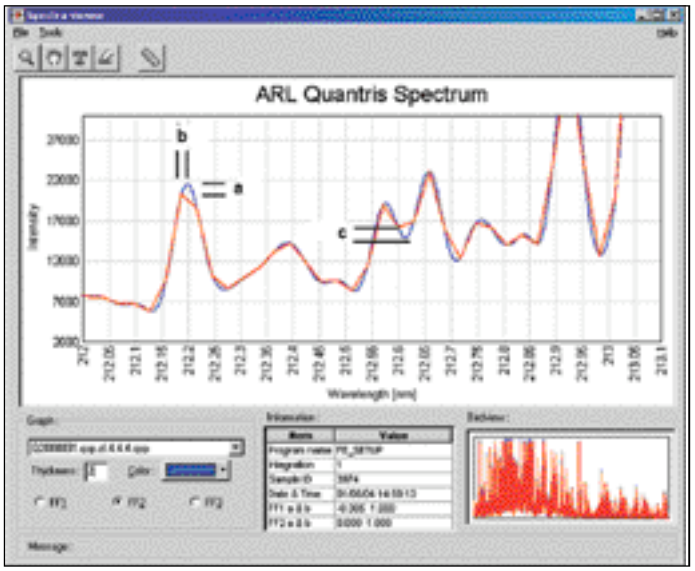

● **Figure 4** ***Comparison between a raw spectrum and a geometrically interpolated spectrum with enhanced digital resolution***

The CCD readings are processed by dedicated powerful 32 bit RISC ARM signal processors and digitised by triple 16 bit A/D converters. The communication with the external PC is done via Fast Ethernet (100Mbit/s) and TCP/IP protocol.

Novel spectrum processing

The pixels of the CCD have a photosensitive layer in which incident photons are detected, and are connected with a potential 'well' where the resulting photoelectrons are collected. At the end of the acquisition period the content of the well is gated out, processed and digitally converted. Elementary acquisition parameters, including the elementary acquisition period, are defined for each CCD and for every matrix, in order to optimise the intensity of lines of interest, while avoiding saturation.

The spectra from each CCD are stored in a file to allow graphical display and are processed to calculate peak intensities or element concentrations. The pixel scale is converted into wavelength range through a calibration function. For each measuring program analytical wavelengths are defined and spectral information is converted into concentrations. Apart from the new architecture of the hardware, real progress in the instrument's performance has been made thanks to mathematical treatment of the spectra.

Several problems had to be overcome by mathematical treatment and measurement strategy:

■ Spectrum 'pixelisation'

Because the pixel acts as a wavelength integrator over the pixel band pass, the spectrum obtained has a histogram shape that may hide details. As a consequence, integration windows for analytical wavelength are difficult to define with high accuracy. *Figure 3a* is an example of a peak with Full Width at Half Maximum (FWHM) of 2.5 pixels.

■ Drift

Drift is unavoidable. With a pixel width of only 7 micrometers, it is sensitive to the drift of the spectrum. *Figure 3b* represents a simulation of drift of the peak displayed in *Figure 3a* of 2 microns, which is equivalent to an 8pm displacement of the spectrum on the second spectrograph.

■ Sensitivity

Typically, the sensitivity of CCD pixels is between one and three orders of magnitude lower than the sensitivity of a PMT. A way to compensate for lower sensitivity is to use the information from more pixels instead of the peak pixel by increasing the active band pass for the analytical window and to reduce the spectral noise. Spectral noise can be defined as pixel flickering as the result of summation of all sources of noise applied to a pixel.

Width of the integration window (pixels)	Peak FWHM VUV spectrograph / Peak FWHM Standard spectrograph	Relative intensity variation for truncation error of 1 pixel (%)	Relative intensity variation for truncation error of 1/4 pixel (%)
7	4	9.5	2.0
	2.5	2.2	0.2
5	4	17.2	3.8
	2.5	10.3	1.5
3	4	32.7	7.7
	2.5	30.7	5.9

● **Table 2** ***Simulation of integrated peak intensity jumps caused by truncation error during drift correction***

Element	SD no filtering	SD with filtering	Improvement factor
Al	1.1	0.5	2.2
C	3.0	1.6	1.9
Cr	5	1.5	3.3
Cu	2	0.5	4
Mn	40	6	6.7
Mo	6	3.2	1.9
N	31	1.6	19.4
Ni	13.5	5	2.5
P	20	2.3	8.7
S	6	1.8	3.3
Si	15	4.8	3.1

● **Table 3** ***Typical improvements by applying digital filtering on pure iron sample 5 RE12***

■ Noise

The CCD detectors and the readout electronics are subject to different type of noise that can be referred to as thermal noise related to thermally generated charges in the CCD structure, photonic or shot noise related to statistical fluctuations of the flux of incident photons, and noise related to the amplifier and signal processor. The thermal noise and the shot noise follow the Poisson law, being expressed as the square root of the number of electrons or photons. Part of the thermal noise is suppressed by cooling the CCD for, as with a silicon structure, the thermal noise doubles every 16°C in the range 0–70°C.

■ Spectral interferences

OES spectra are very complex and, depending on

ELEMENT	Al	B	Bi	C	Ca	Ce	Co	Cr	Cu
DL [ppm]	6.3	1.2	9	6.2	0.8	28	15	6	4.5
Precision level %	SD	SD	SD	SD	SD	SD	SD	SD	SD
0.001		0.00002			0.00002				0.0001
0.005	0.00015	0.00006	0.0002	0.0002	0.0002		0.0003	0.00025	0.00015
0.01	0.00015	0.0001	0.00025	0.0003	0.0004	0.0007	0.0003	0.0003	0.00015
0.05	0.0003	0.0005	0.00065	0.0005		0.001	0.0005	0.00035	0.0003
0.1	0.0004	0.001	0.0011	0.0007		0.0015	0.0008	0.0005	0.00045
0.5	0.0015	0.005		0.002			0.003	0.0015	0.002
1	0.003	0.01		0.004			0.005	0.003	0.0035
5				0.017			0.032	0.009	0.016
10							0.085	0.015	
20								0.03	
40								0.06	

ELEMENT	La	Mg	Mn	Mo	N	Nb	Ni	P	Pb
DL [ppm]	8.5	0.7	25	30	16	10	20	20	13
Precision level %	SD	SD	SD	SD	SD	SD	SD	SD	SD
0.001		0.00002							
0.005	0.00025	0.0001		0.0008	0.0005	0.0004	0.0005	0.0004	0.0004
0.01	0.0004	0.0002	0.0008	0.0008	0.00055	0.0004	0.0005	0.0005	0.00075
0.05	0.0016	0.0015	0.0009	0.001	0.00075	0.0007	0.0007	0.0008	0.003
0.1	0.0030	0.0035	0.0011	0.0015	0.001	0.001	0.0009	0.0015	
0.5			0.0025	0.004	0.005	0.004	0.002	0.007	
1			0.0045	0.007	0.02	0.009	0.004	0.02	
5			0.020	0.04		0.09	0.014		
10			0.045	0.10			0.025		
20			0.10				0.05		
40							0.09		

Element	S	Sb	Si	Sn	Ti	V	W	Zn	Zr
DL [ppm]	13	5	18	10	6	15	150	6	11
Precision level %	SD	SD	SD	SD	SD	SD	SD	SD	SD
0.001									
0.005	0.0003	0.00015	0.0004	0.00025	0.0002	0.0005		0.0002	0.0003
0.01	0.0004	0.0003	0.0004	0.00025	0.0003	0.0005		0.00025	0.0004
0.05	0.001	0.0007	0.0005	0.0005	0.00065	0.0007	0.0035	0.0008	0.001
0.1	0.002	0.001	0.0007	0.001	0.001	0.001	0.004		0.002
0.5			0.002		0.005	0.003	0.006		0.01
1			0.0035		0.01	0.006	0.01		
5			0.017			0.03	0.03		
10						0.06	0.06		
20							0.13		
40									

● **Table 4** ***ARL QUANTRIS detection limits (3 sigma) and typical precision values (1 sigma) for iron base***

matrix and sample excitation parameters, between 20,000 and 30,000 lines are visible in the range of 130–780nm. Original and robust treatments have been successfully applied to the ARL QUANTRIS spectra, leading to top analytical performance. Each of these treatments solves one of the above problems, but the final effects are interconnected.

■ Enhancement of numerical resolution

An original mathematical treatment for numerical resolution enhancement was developed for ARL QUANTRIS. The treatment corresponding to a geometrical interpolation enhances the numerical resolution by reducing the step dimension of the spectrum. *Figure 4* shows a comparison between a raw spectrum and a geometrical interpolated spectrum with a numerical resolution enhancement factor of 4 (ie, numerical resolution is 0.25 pixel after treatment). The numerical resolution enhancement improves accuracy in peak intensity, peak position and spectral resolution. The letters indicate the accuracy improvement for the peak intensity (a), peak position (b) and resolution (c).

■ Drift correction

The peak positions of well-defined and resolved lines, computed by special peak-fitting algorithms, are compared to reference positions on the CCDs. The drift correction algorithm moves and deforms the spectrum in order to find the smallest differences with the reference lines. By introducing numerical resolution enhancement, the accuracy of drift correction increases and consequently the intensity jumps as the problem of rounding to the nearest pixel diminishes. *Table 2* shows the results of simulations of the intensity jumps due to truncation, for various symmetrical integration windows on two peaks (the integration windows are symmetrical and centred on the peak pixel): one situated on the VUV spectrograph, with a FWHM of 4 pixels, the second situated on the standard spectrograph with FWHM of 2.5 pixels.

■ Spectrum noise reduction

Several low-pass digital filters were adopted on the ARL QUANTRIS. The filters are matched to the characteristics of the spectral region of interest through resolution and integration window width. Digital filtering improves reproducibility and lowers the detection limits. *Table 3* shows the typical improvements for a pure iron sample 5RE12, expressed as standard deviations (SD) obtained on 10 measurements, without and with filtering.

■ Flexible intensity computation

Calculating the line intensity by summation over an integration window increases CCD sensitivity so window widths are rigorously selected in order to minimise spectral overlaps. Off peak and on peak background subtractions are implemented for selected lines in order to lower detection limits and to compensate for interferences. One of the biggest advantages of having the whole spectrum available is

the capability to select for each analytical line, the best-suited internal standard line that behaves similarly and compensates for the instrumental changes. By selecting homologous-type internal standard lines, reproducibility is increased by a factor of 2 to 4. This is clearly a strong advantage over PMT instruments, where the number of available lines is limited. For the iron base, 14 carefully tested internal standard lines are selected, providing excellent performance.

Detection limits and precision

Table 4 shows the actual performances obtainable for analysis needed in the steel industry. The detection limits (DL) and the typical precision levels are similar to those attainable with PMT instruments.

The instrument can be factory calibrated for numerous variants of the iron matrix, such as low alloy steels, Cr-Ni steels, Cr steels, cast and nodular iron, high speed and tool steels.

Conclusions

Thanks to the new hardware concept and the novel spectrum treatment, the ARL QUANTRIS bridges the performance gap between CCD and PMT instruments.

Even if the resolution is limited and the sensitivity of the CCD detector is lower in comparison to PMT instruments, the full spectrum coverage and the adopted numerical methods generate very good detection limits that satisfy most of the analytical demands in the steel industry, and offer an equivalent or superior precision for the measurement of key alloying elements. Moreover, it works as a multi-matrix instrument, with unlimited applications, for production and development.

Emile Muller is Technical Director OES, Software & Automation, Jean-Marc Böhlen is Manager OES Applications and Edmund Halász is Application Specialist OES at Thermo Electron in Ecublens, Switzerland.